The unusual conduction band structure of Ga(AsN) probed by magneto-tunnelling and

photocurrent spectroscopy

# The unusual conduction band structure of Ga(AsN) probed by magneto-tunnelling and photocurrent spectroscopy

**A Patanè, J Endicott, J Ibáñez and L Eaves**

School of Physics and Astronomy, University of Nottingham, Nottingham NG7 2RD, UK

**Abstract**

We use a combination of magneto-tunnelling and photocurrent spectroscopy techniques to explore the admixing of the extended GaAs conduction band states with the localized N impurity states in dilute $GaAs_{1-y}N_y$ quantum wells (QWs) with $y < 2\%$. We show that the current–voltage $I(V)$ characteristics of our resonant tunnelling diodes are profoundly affected by the incorporation of N. For a small N content ($y = 0.08\%$), electron tunnelling into the N-induced $E_-$ and $E_+$ hybridized subbands of the $GaAs_{1-y}N_y$ QW layer leads to two main resonances in $I(V)$. Magneto-tunnelling spectroscopy provides us with a powerful means of probing the energy–wavevector $\varepsilon(k)$ dispersion curves of the $E_-$ and $E_+$ subbands. We find that $E_-$ and $E_+$ have a very well defined character and that the heavy effective mass $E_+$ states have a significant $\Gamma$ conduction band character even at $k = 0$. In the devices with larger $y$-values ($y > 0.08\%$) the resonances are smeared out and the measured currents are much smaller. This is attributed to the disorder in the QW and carrier trapping on localized N levels, which break the momentum conservation condition required for observing sharp resonances in $I(V)$. The current resonances can be partially recovered by optical excitation due to the effect on the current of photocreated holes that recombine with majority electrons tunnelling in resonant states of the QW. This photoinduced current enhancement depends on the optical absorption of the $GaAs_{1-y}N_y$ QW and provides a means of measuring the energy position of the valence to $E_-$ subband transition at various $y$-values. Our study indicates that although the $E_-$ subband states are significantly energy broadened due to disorder effects, their energy position is well described by a band anticrossing model.

## 1. Introduction

The electronic properties of GaAs are profoundly affected by the incorporation of low concentrations of N [1–3]. A reduction of the band-gap of about 0.1 eV per atomic per cent of N

content has been observed in $GaAs_{1-y}N_y$ for $y < 2\%$. This has raised the interesting possibility of using N-containing alloys grown on GaAs substrates for long wavelength optoelectronic applications. At present, research on $GaAs_{1-y}N_y$ represents one of the most active topics in semiconductor physics. In the ultra-dilute regime ($y < 0.01\%$), N introduces a single-impurity level at an energy of $\sim 0.2$ eV above the conduction band minimum of GaAs [4]. At higher values of $y$, the electronegativity of the N atoms combined with the stretching and compressing of neighbouring bonds results in a strong perturbation of the host crystal, which has significant effects on the band structure properties of $GaAs_{1-y}N_y$. According to band anticrossing (BAC) models [5, 6], the interaction of the extended $\Gamma$ conduction band states of GaAs with the localized N energy level causes a splitting of the conduction band into two subbands $E_-$ and $E_+$, which have been observed experimentally by many groups [5, 7]. Pseudopotential calculations [8, 9] and tight-binding models [10] clearly reveal that the $E_-$ and $E_+$ subbands are strongly admixed: the strong perturbation of the host crystal caused by N gives rise to an admixing of the $\Gamma$ states with states from the higher energy L and X conduction bands and to the formation of the hybridized subbands, $E_-$ and $E_+$, as well as to additional states [8, 9]. Close to its energy minimum at wavevector $k = 0$, the character of $E_-$ is predominantly that of the $\Gamma$ conduction band but it has a significant admixing of states from the L conduction band minima. The upper $E_+$ is predominantly L-like and acquires an increasing $\Gamma$ character as $y$ is increased. The coexistence of different local environments in the alloy also complicates the electronic properties of $GaAs_{1-y}N_y$ [8, 9]: single N impurities form perturbed delocalized states in the host lattice, whereas N aggregates, such as impurity N–N pairs and higher order clusters, form strongly localized states; these two different types of states form a so-called 'amalgamated' conduction band, thus leading to a duality of band-like and localization behaviours for electrons.

Surprisingly, despite the great topical interest in dilute nitrides and their potential for use in novel electronic devices, most of the experimental works published in the current literature focus on the optical properties of $GaAs_{1-y}N_y$ [7]. In contrast, little is known about the possibility of integrating the new material systems in a number of relevant heterostructure devices, such as resonant tunnelling diodes (RTDs) [11]. In recent papers [12, 13], we have shown that magneto-tunnelling spectroscopy (MTS) can provide us with a powerful means of exploring the admixing of the extended conduction band states of GaAs with the localized N impurity states. In particular, the MTS technique allow us to probe fundamental electronic properties of $GaAs_{1-y}N_y$, such as energy–wavevector dispersion curves [12] and wavefunction probability densities [13], as has already been done for other semiconductor material systems [14–16]. These studies are also central to the exploration of the potential of dilute nitrides for novel band structure engineered devices. For example, according to band anticrossing models [5, 6], the lowest energy subband $E_-(k)$ has an inflection point, corresponding to a maximum electron velocity, at relatively modest wavevectors $k$, considerably smaller than the size of the Brillouin zone. At energies above this point, the subband has a region with negative effective mass. This property could be exploited in devices in which electrons are accelerated by an electric field up to and beyond their peak velocity, thus leading to non-linear electrical conduction, analogous to that occurring in Gunn diodes and superlattices [17, 18].

In this work we present a detailed study of the transport and optical properties of resonant tunnelling diodes based on the $GaAs/Al_{0.4}Ga_{0.6}As/GaAs_{1-y}N_y$ heterostructure system. We show that the current–voltage characteristics of our tunnelling diodes are profoundly affected by the incorporation of N. When $y$ is increased from 0 to 0.08%, the current resonance due to electrons tunnelling through the lowest quasi-bound state of the $Al_{0.4}Ga_{0.6}As/GaAs_{1-y}N_y$ quantum well (QW) splits into two main components due to electron tunnelling into the N-

induced $E_-$ and $E_+$ hybridized subbands of the GaN$_y$As$_{1-y}$ QW layer. We use magneto-tunnelling spectroscopy to probe the energy–wavevector $\varepsilon(k)$ dispersion curves of the $E_-$ and $E_+$ subbands. Our data reveal that for $y = 0.08\%$, $E_-$ and $E_+$ have a very well defined character and that the heavy effective mass $E_+$ states have a significant $\Gamma$ conduction band character even at $k = 0$. These measurements also demonstrate that at small $y$ the admixing of the extended GaAs conduction band states with the localized N impurity states is well described by a band anticrossing model [5, 6]. In contrast, in the devices with larger $y$-values ($y > 0.08\%$) the resonances are smeared out and the measured currents are much smaller. This is attributed to the disorder in the QW and carrier trapping on localized N levels, which break the momentum conservation condition required for observing clear resonances in $I(V)$. The resonances in $I(V)$ can be partially recovered by optical excitation due to the effect on the current of photocreated holes that recombine with majority electrons tunnelling in resonant states of the QW. This photoinduced current enhancement depends on the optical absorption of the GaAs$_{1-y}$N$_y$ QW layer and provides a means of probing the conduction band. These studies clearly indicate that the optical absorption of GaAs$_{1-y}$N$_y$ at high $y$ is dominated by interband transitions involving the $E_-$ subband states, which are energy broadened due to disorder effects.

## 2. Samples and experiment

Our samples were grown by MBE on (100)-oriented n-type GaAs substrates. In our structures, an 8 nm thick GaAs$_{1-y}$N$_y$ ($y = 0$, 0.08, 0.43, 0.93 and 1.55%) quantum well layer is embedded between two 6 nm thick Al$_{0.4}$Ga$_{0.6}$As tunnel barriers. Undoped GaAs spacer layers, each of width 50 nm, separate the Al$_{0.4}$Ga$_{0.6}$As barriers from n-doped GaAs layers in which the doping concentration is increased from $2 \times 10^{17}$ cm$^{-3}$, close to the barrier, to $2 \times 10^{18}$ cm$^{-3}$. The thicknesses of these two n-doped GaAs layers are 50 and 500 nm, respectively. The samples were processed into circular mesas with diameters between 25 and 400 $\mu$m, with a ring shaped top contact to allow optical access for current–voltage $I(V)$ measurements under illumination, photoluminescence (PL) and photocurrent (PC) studies. For the PL measurements, the diode was excited with a He–Ne laser. The PL was dispersed by a 1/2 m monochromator and detected by an (InGa)As detector. The excitation source for the PC measurements was a tungsten–halogen lamp, dispersed by a 0.25 m monochromator, and the PC signal was recorded using standard lock-in techniques. For the $I(V)$ measurements under illumination, the diode was excited either with a He–Ne laser or with a tungsten–halogen lamp. Capacitance–voltage $C(V)$ measurements were made with an HP 4275A LCR meter over the frequency range 10 kHz–1 MHz.

## 3. Photoluminescence of dilute nitride QWs

The low temperature ($T = 4.2$ K) PL spectra of our RTDs show an emission band that shifts to low energy with increasing N content (see figure 1). This is attributed to electron–hole recombination from states of the GaAs$_{1-y}$N$_y$ QW. The $y$-dependence of the energy position of the PL emission (see inset of figure 1) is similar to that reported by other groups for similar GaAs$_{1-y}$N$_y$ samples [7] and confirms that the electronic properties of our structures are profoundly affected by the incorporation of low N concentrations. However, although PL studies can clearly reveal the effect of N on the electronic properties of GaAs$_{1-y}$N$_y$, they do not provide detailed information about the admixing of the extended conduction band states of GaAs with the localized N impurity states and the nature, impurity-like or band-like, of
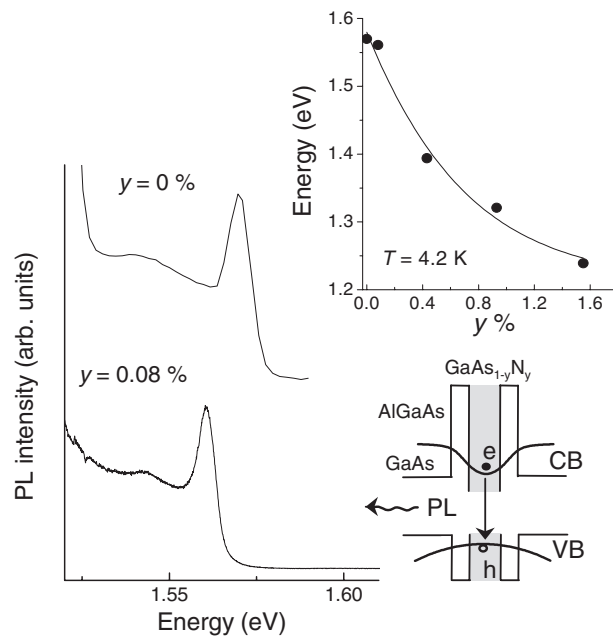
**Figure 1.** PL spectra at $T = 4.2$ K for samples with $y = 0$ and $0.08\%$. These show a sharp emission band peaked at 1.57 eV ($y = 0$) and 1.56 eV ($y = 0.08\%$) due to electron–hole recombination in the GaAs$_{1-y}$N$_y$ QW layer. The PL emission observed at lower energies originates from electron–hole recombination in the GaAs-doped layers of the RTD. The top inset shows the energy position of the PL band due to N-related states in the GaAs$_{1-y}$N$_y$ QW as a function of $y$ ($T = 4.2$ K). The bottom inset sketches the electron–hole recombination in the GaAs$_{1-y}$N$_y$ QW layer.

the N levels. In fact, the low temperature PL spectra are very often dominated by interband transitions involving localized N-related defects and cluster states and do not provide a direct description of the density of states in the conduction band of GaAs$_{1-y}$N$_y$. We show in the next section how tunnelling and photocurrent spectroscopy can complement the PL data and allow us to probe in detail the unusual conduction band structure of GaAs$_{1-y}$N$_y$.

## 4. Tunnelling through dilute nitride QWs

The inset of figure 2 shows schematically the conduction band profile of our RTDs. When a voltage is applied, resonant tunnelling through a particular state in the GaAs$_{1-y}$N$_y$ QW layer gives rise to a peak in $I(V)$, whenever this state is resonant with an adjacent filled state in the negatively biased electron emitter layer. As shown in figure 2, when we compare the $I(V)$ curves of the control sample ($y = 0$) and of the sample with nitrogen content $y = 0.08\%$ in the QW, we find that the resonance $E_0$ due to electrons tunnelling through the lowest quasi-bound state of the QW splits into two main resonant features, $E_{0-}$ and $E_{0+}$, due to the presence of N. These components can be seen more clearly in the $I(V)$ measured under illumination (see dashed line in figure 2). In contrast, further increase of $y$ smears out the resonances, strongly quenches the current and shifts to higher biases the threshold voltage at which the current increases rapidly (see figure 3).

The $I(V)$ curves clearly indicate that N incorporation has strong effects on the electron tunnelling dynamics. This is not unexpected as the energy levels of the GaAs QW layer
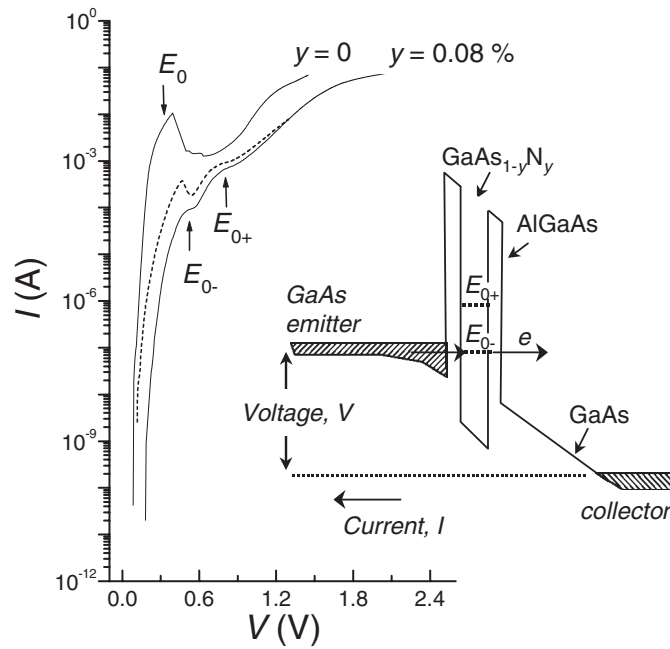
**Figure 2.** $I(V)$ curves at $T = 4.2$ K for RTDs incorporating $GaAs_{1-y}N_y$ layers with $y = 0$ and 0.08%. The dashed line is the $I(V)$ under illumination for the sample with $y = 0.08\%$ (from [12]). The inset sketches the conduction band profile of our RTDs under applied bias.

are profoundly changed by N incorporation. According to band anticrossing models [5, 6], the interaction of the extended conduction band states of GaAs with the localized nitrogen levels induces a splitting of the conduction band into two subbands $E_-$ and $E_+$ (figures 3(b) and (c)). These are likely to be responsible for the $E_{0-}$ and $E_{0+}$ resonances observed in the sample with $y = 0.08\%$. N incorporation also leads to formation of N cluster states and N-related defects with associated energy levels below the GaAs conduction band edge [8, 19, 20], which can affect strongly the conduction band profile of our tunnel diodes (figure 3(d)) and the corresponding $I(V)$ characteristics. At zero bias, equilibrium is established by electrons diffusing from the doped GaAs layers into the N-induced localized states in the $GaAs_{1-y}N_y$ QW layer. Negative charge in the well gives rise to two depletion layers in the regions beyond the $Al_{0.4}Ga_{0.6}As$ barriers and a corresponding band bending that inhibits the current flow at low voltages. The monotonic shift to higher biases of the $I(V)$ curve with increasing $y$ is consistent with an increasing negative charge in the well due to formation of deeper low energy N states in the $GaAs_{1-y}N_y$ layer. This charging effect was studied in detail by capacitance–voltage $C(V)$ measurements.

Figure 4(a) shows the $C(V)$ curves at $T = 4.2$ K for three RTDs with $y = 0$, 0.08 and 0.93%. The capacitance is defined as $C = dQ/dV$, where $dQ = -dQ_{em} - dQ_{QW} = dQ_{dep}$ is the incremental change of the negative charge in the emitter layer ($dQ_{em}$) and in the QW ($dQ_{QW}$) for an incremental change in the applied voltage $dV$. The corresponding increase in the positive charge in the collector depletion layer is $dQ_{dep}$ [21, 22]. In the RTD with $y = 0\%$, the capacitance rises at a relatively low bias since an accumulation layer quickly forms in the emitter side of the device. In contrast, the $C(V)$ curves of samples with $y > 0\%$ show an almost constant capacitance ($\sim$26 pF) over an extended voltage range between zero bias
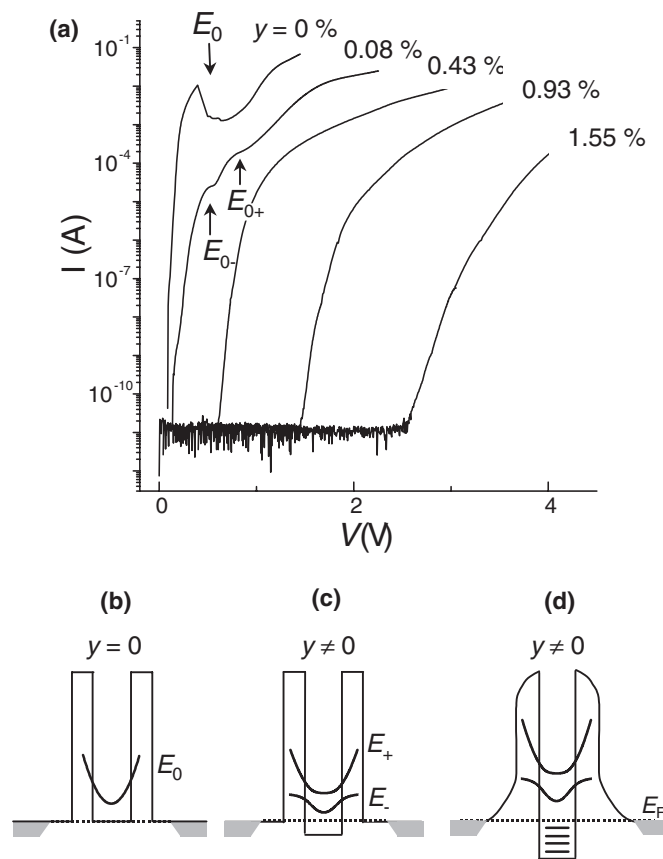
**Figure 3.** (a) $I(V)$ curves at $T = 4.2$ K for RTDs incorporating a GaAs$_{1-y}$N$_y$ layer. ((b)–(d)) Sketches of the conduction band profile at zero bias for RTDs with and without N (from [12]). In the presence of N, the lowest subband of the QW, $E_0$, splits into two subbands, $E_-$ and $E_+$ ((c) and (d)). Also N incorporation leads to the formation of N cluster and N-related defects with energies below the continuum of band-like states, which act as traps of electrons. Negative charge in the well gives rise to two depletion layers in the regions beyond the Al$_{0.4}$Ga$_{0.6}$As barriers and a corresponding band bending ((d)).

and the threshold voltage $V_{th}$. This value of capacitance is consistent with the separation $d$ between the edges of the two doped GaAs layers ($d \sim 120$ nm).[1] For $V > V_{th}$ the capacitance increases rapidly. Note that the value of $V_{th}$ is also quite close to the bias value at which the current increases sharply. This behaviour can be explained by the fact that at zero bias electrons accumulate in the QW, and depletion layers form in the nominally undoped GaAs region beyond the Al$_{0.4}$Ga$_{0.6}$As barriers. This gives rise to a relatively wide region of dielectric containing no free carriers. At zero bias, the positive charge associated with each depletion layer is equal to half the negative charge in the QW layer ($Q_{QW}$). Therefore a significant applied voltage ($\sim V_{th}$) is required to start filling with electrons the GaAs layer adjacent to

[1] We model the diode as a parallel plate capacitor with capacitance $C = \varepsilon_0 \varepsilon_r A/d$, where $\varepsilon_0$ is the permittivity constant in vacuum, $\varepsilon_r$ is the relative permittivity of GaAs, $A$ is the area of the mesa and $d$ is the distance between the fronts of the free carrier regions on the emitter and collector sides of the device. From the $C(V)$ curve of sample with $y = 0.08\%$, we estimate that $d$ varies from 140 to 100 nm for $V$ increasing from 0 V to biases close to the voltage position of the current resonances in $I(V)$.
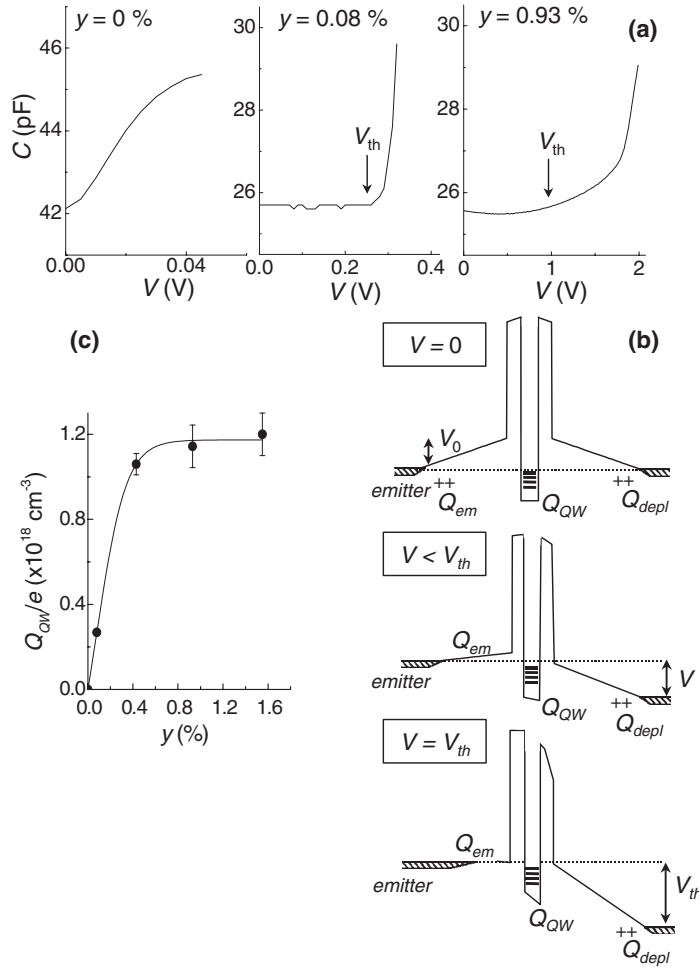
**Figure 4.** (a) $C(V)$ characteristics at $T = 4.2$ K for the RTDs with $y = 0$, 0.08 and 0.93% for a mesa of radius $r = 100$ $\mu$m. $V_{th}$ indicates the threshold voltage for the increase of capacitance. (b) Sketches of the potential profile for RTDs containing N for $V = 0$ V, $V < V_{th}$ and $V = V_{th}$. (c) The dependence on N content of the volume density of electrons trapped in the $GaAs_{1-y}N_y$ QW layer, $Q_{QW}/e$.

the emitter barrier and hence to increase the capacitance. As sketched in the band diagram of figure 4(b), $V_{th}$ is the applied voltage required to reach flat band conditions on the emitter side of the device. In particular, assuming that the negative charge in the QW layer ($Q_{QW}$) does not change between $V = 0$ and $V_{th}$, the value of $Q_{QW}$ is determined using the relation $\int_0^{V_{th}} C \, dV = C_0 V_{th} = \int_0^{V_{th}} dQ_{depl} \sim Q_{QW}/2$, where $C_0$ is the constant value of capacitance measured for $V < V_{th}$. Using the experimental values of $C_0$ and $V_{th}$, we estimate that the volume density of electrons trapped in the well is $Q_{QW}/e = 2C_0 V_{th}/e\pi L r^2 = 2.6 \times 10^{17}$, $1.06 \times 10^{18}$, $1.14 \times 10^{18}$ and $1.2 \times 10^{18}$ cm$^{-3}$ for samples with $y = 0.08, 0.43, 0.9$ and $1.55\%$, respectively, where $r = 100$ $\mu$m is the radius of the mesa and $L = 8$ nm is the well width. The increasing negative charge in the $GaAs_{1-y}N_y$ QW with increasing $y$ (see figure 4(c)) indicates an increasing degree of alloy fluctuations and formation of N clusters and N-related defects with associated localized levels charged with electrons. The density of these localized states is

much smaller than the nominal density of isolated N atoms ($>10^{19}$ cm$^{-3}$), but can give rise to appreciable scattering of tunnelling electrons and is likely to be responsible for the smearing of the current resonances at large $y$. In the absence of disorder, both the energy and the in-plane component of the momentum of a tunnelling electron are conserved; these are the conditions required for observing a sharp peak and the associated negative differential conductance in the $I(V)$ curve [11]. The destruction of translational symmetry due to the disordered QW potential tends to break the momentum conservation condition and smears out the resonances, as is observed even for $y = 0.08\%$. The resonances observed in the $I(V)$ of this sample can be enhanced by optical excitation (see figure 2). As discussed below, we attribute this enhancement to the effect of screening of the disorder in the QW by the photogenerated holes and to the effect on the current of hole recombination with majority electrons tunnelling in resonant states of the QW.

## 5. Photocurrent spectroscopy studies

Figure 5 illustrates the dynamics of carriers when the device is excited with light of energy larger than that of the GaAs band-gap. Electrons are electrically injected from the negatively biased GaAs emitter layer into the well. At the same time, light creates photocarriers in the GaAs layers. The electric field in the electron depletion layer (on the right-hand side of the barrier in figure 5) separates the oppositely charged carriers created in this region: the photoelectrons are swept into the positively biased electron collector, whereas the holes are attracted by the negatively biased electron emitter and form an accumulation layer adjacent to the right-hand tunnel barrier. During resonant transmission of electrons and photogenerated holes through the well, some of the electrons can recombine with the holes. In turn this affects the tunnel current. The emptying of N-related states by the holes leads to an increase in the number of electrons that tunnel into the QW and to a corresponding enhancement of the current resonances in $I(V)$ as clearly observed for $y = 0.08\%$ (see figures 2 and 5(b)). For this sample, it is likely that the photocreated holes act also to partially screen the disordered potential of the QW and restore the momentum conservation condition required for observing clear current resonances in $I(V)$. In contrast, for $y > 0.08\%$, the optical excitation produces a general increase of current but does not reveal resonances in $I(V)$. For each sample with $y > 0.08\%$, only a broad peak in the photoinduced current can be observed (see figure 5(b)); the bias position of this peak increases with increasing $y$. We attribute this broad photoinduced peak in the current to the effect of holes on electrons tunnelling through states of the broadened conduction band of the GaAs$_{1-y}$N$_y$ layer. When an electron tunnels through the two barriers non-resonantly, its dwell time in the QW is given approximately by the time for a single transit of electrons across the well. Since this time is very short ($<1$ ps), it is unlikely that electrons can recombine with the holes. Therefore, the current of majority electrons tunnelling though the QW is weakly affected by light and the photoinduced current is small. In contrast, when an electrons tunnels resonantly into a bound state of the QW, its dwell time is much longer, which leads to a larger probability for recombination with the holes and hence to a larger photocurrent signal.

Figure 6(a) shows the dependence on the light excitation energy, $h\nu_{exc}$, of the PC intensity at an applied bias corresponding to the current peak in the PC($V$) curve of each sample. The low temperature ($T = 4.2$ K) PC spectra of all structures clearly reveal a current enhancement for $h\nu_{exc} > 1.5$ eV, which corresponds to carriers photocreated in the GaAs layers on each side of the barriers and QWs. The PC spectra also reveal a weaker band that shifts to low energy with increasing amount of N (see the vertical arrow in figure 6). We assign this to the effect on the tunnel current of holes photocreated in the GaAs$_{1-y}$N$_y$ QW layer. This photoinduced
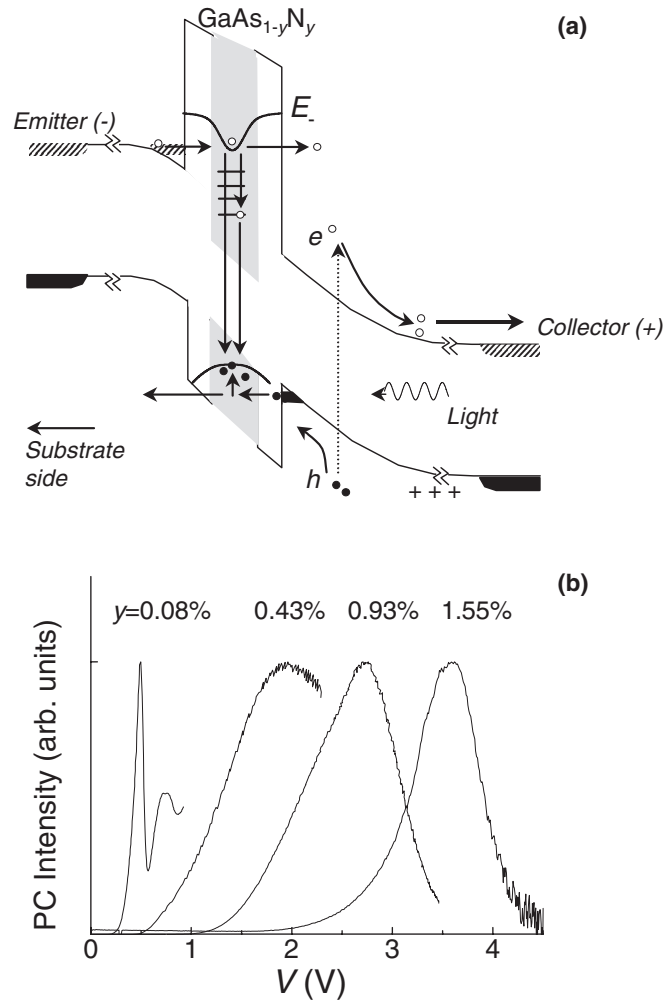
**Figure 5.** (a) A sketch of the potential profile and carrier dynamics for a RTD in forward bias (negative biased substrate) with above-band-gap illumination. (b) The PC intensity versus the applied bias for RTDs containing N. Each diode was excited with above-band-gap laser light (633 nm) and power densities $\sim$0.1 W cm$^{-2}$. The shape of the PC($V$) curves is not affected by the level of illumination.

current enhancement depends on the optical absorption of the QW and provides us with a means of investigating the conduction band states of GaAs$_{1-y}$N$_y$.

We use a band anticrossing model to estimate the energy position of the $E_-$ QW subband states. For bulk GaAs$_{1-y}$N$_y$, the $E_-$ subband is calculated using the relation $E_-(k) = \frac{1}{2}[(E_M(k) + E_N) - \sqrt{(E_M(k) - E_N)^2 + 4yC_{MN}^2}]$, where $E_M(k)$ is the energy–wavevector dispersion curve of the conduction band of GaAs around $k = 0$, $E_N$ is the energy position of the N-related level ($E_N = 1.725$ eV and we assume that is independent of temperature) and $C_{MN}$ is the hybridization matrix element ($C_{MN} = 2.7$ eV) [5]. For the case of the GaAs$_{1-y}$N$_y$/Al$_{0.4}$Ga$_{0.6}$As QW, we use the same relation but with $E_M(k)$ replaced by the energy–wavevector dispersion curve for the lowest energy subband of the QW. As shown
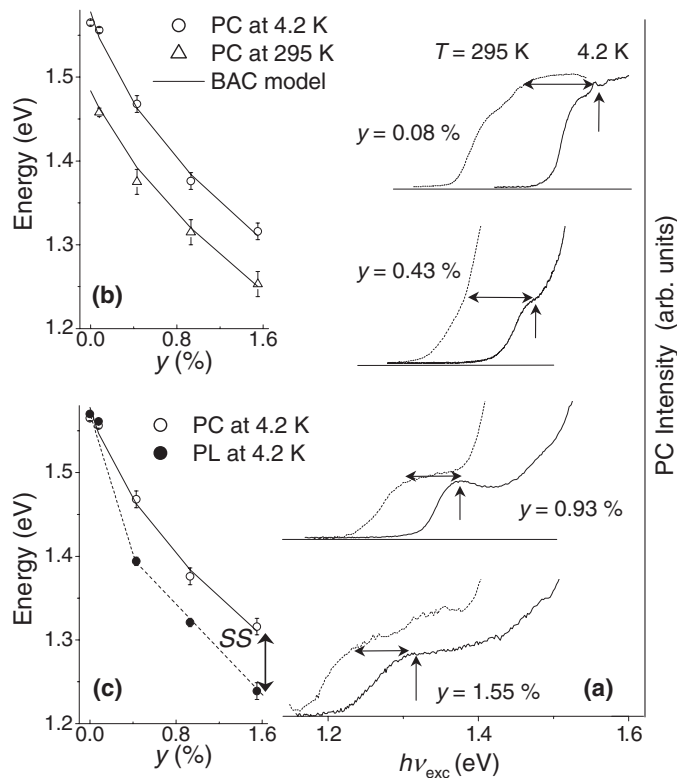
**Figure 6.** (a) PC spectra at 4 and 295 K for RTDs with $y = 0.08$, 0.43, 0.93 and 1.55%. Each diode was biased at voltages corresponding to the current peak in the PC($V$) curves shown in figure 5(b). The vertical and horizontal arrows indicate the energy position of the N-related absorption line at $T = 4.2$ K and the corresponding thermal shift when $T$ is increased to 295 K. (b) The energy dependence of the peak in intensity of the N-related PC band at 4.2 and 295 K. Continuous curves show the calculated energies for the interband transition between the quantized electron and hole levels of the QW at 4.2 and 295 K. The circles and triangles are data points. (c) The energy dependence of the energy peak of the N-related PC and PL bands at 4.2 K. The dotted line is a guide to the eye. The continuous line is the calculated energy for the interband transition between the quantized electron and hole levels of the QW at 4.2 K. The vertical arrowed line represents the Stokes shift between the PC and PL bands.

in figure 6(b), the dependence on $y$ of the energy of the transition between the quantized electron $E_-$ states predicted by the BAC model and heavy hole levels of the QW describes well our low temperature PC data. The BAC model also accounts for the energy shift of the N-related PC feature when $T$ is increased from 4.2 to 295 K. However, the BAC model cannot explain the energy position of the PL emission, which shows a significant energy red-shift with respect to the PC absorption, referred to as the Stokes shift, SS (see figure 6(c)). The increasing value of SS with increasing $y$ and the corresponding energy broadening of the PC spectrum indicate the existence of a broad energy distribution of N-related localized states in the vicinity of the $E_-$ subband edge. It seems likely that the strong dependence of the conduction band minimum on N content creates large variations in the electron energy due to statistical compositional alloy fluctuations. Also N clusters form strongly localized levels. These states admix together to form an 'amalgamated' broadened conduction band [8]. In a PL experiment, carriers relax into the lowest energy levels before recombining. Therefore, the PL is often dominated by

transitions involving N-related localized states and is red-shifted with respect to the absorption spectrum. According to the simple model for the Stokes shift of [23], if the disorder extends over a scale much larger than the carrier diffusion length, carriers relax into local minima before recombining. In particular, in the presence of a distribution of energy levels of full width at half-maximum $W$, the PL reflects the distribution of local minima and $SS = 0.55W$. Our PC data suggest energy broadening as large as $W \sim 100$ meV for $y > 0.08\%$, which corresponds to a value of SS of 55 meV consistent with the large SS obtained from comparing the PL and PC data. These studies clearly indicate that the optical absorption of $GaAs_{1-y}N_y$ at high $y$ is dominated by interband transitions involving the $E_-$ subband states, which are energy broadened due to disorder effects for $y > 0.08\%$. The disorder in the QW and carrier trapping on localized N levels break the momentum conservation condition required for observing sharp resonances in $I(V)$ and explains the strong quenching of current and smearing of the resonances in $I(V)$ at high $y$.

## 6. Magneto-tunnelling spectroscopy

In this section we describe how magneto-tunnelling measurements can provide further detailed information about the nature of the $E_-$ and $E_+$ subbands of the $GaAs_{1-y}N_y$ QW layer [12]. The experiments also provide a test of the BAC model. In these experiments, a magnetic field, $B$, is applied parallel to the QW plane $(X, Y)$. For $y > 0.08\%$, the energy position and amplitude of the resonances in the $PC(V)$ plots are almost unaffected by the magnetic field up to the available field of 12 T. This suggests that they arise from tunnelling of electrons through localized N-related states as was also observed for similar RTDs with $y \sim 2\%$ [13]. The broad energy distribution of N levels revealed by the PC spectroscopy study also supports this description. In contrast, resonances $E_{0-}$ and $E_{0+}$ in the $I(V)$ plot of the RTD with $y = 0.08\%$ are strongly affected by $B$. Figures 7(a) and (b) show the $B$-dependence of the $I(V)$ plots under illumination for $y = 0.08\%$. An identical $B$-dependence of the resonant peaks in the $I(V)$ curves was also measured in dark conditions. The data show a shift to higher bias of $E_{0-}$ and $E_{0+}$ and a general increase of current with increasing $B$. However, the relative weight of $E_{0-}$ and $E_{0+}$ changes significantly with $B$. The $B$-dependence of the amplitude of the $E_{0-}$ and $E_{0+}$ peaks in $I(V)$ has the characteristic form of a quantum mechanical admixing effect, i.e. with increasing $B$, the $E_{0-}$ feature tends to become weaker and disappear whereas the $E_{0+}$ peak increases significantly in amplitude. Also, the $I(V)$ curves show a further weak feature $(E^*)$, which shifts to higher bias with increasing $B$ and disappears for $B > 6$ T. This feature is more clearly revealed in the differential conductance plot shown in figure 7(c). By carrying out a series of measurements for different orientations of $B$ in the (100) growth plane, we find that both the intensity and bias position of the resonances are isotropic.

We can understand the $B$-dependence of the resonances in terms of the effect of $B$ on an electron tunnelling into the states of the $GaAs_{1-y}N_y$ QW. Let $\alpha$, $\beta$ and $Z$ indicate, respectively, the direction of $B$, the direction normal to $B$ in the growth plane and the normal to the tunnel barrier. Due to the action of the Lorentz force, when an electron tunnels from the emitter into the well, it acquires an additional in-plane momentum given by $k_\beta = eBs/\hbar$, where $s$ is the tunnelling distance from the emitter to the QW. Varying $B$ allows us to tune an electron to tunnel into a given $k_\beta$ state of the well; the voltage tunes the energy so that by measuring the voltage position of the peaks in $I(V)$ as a function of $B$, we can map out the energy–wavevector dispersion curve $\varepsilon(k_\beta)$ of the $GaAs_{1-y}N_y$ QW layer.

Figure 8(a) shows the $B$-dependence of the voltage position of the current features $E_{0-}$, $E_{0+}$ and $E^*$. The $V(B)$ plots for $E_{0-}$ and $E_{0+}$ resemble the dispersion curves $\varepsilon(k)$ of the $E_-$ and $E_+$ subbands calculated by using a two-band anticrossing model of bulk $GaAs_{1-y}N_y$
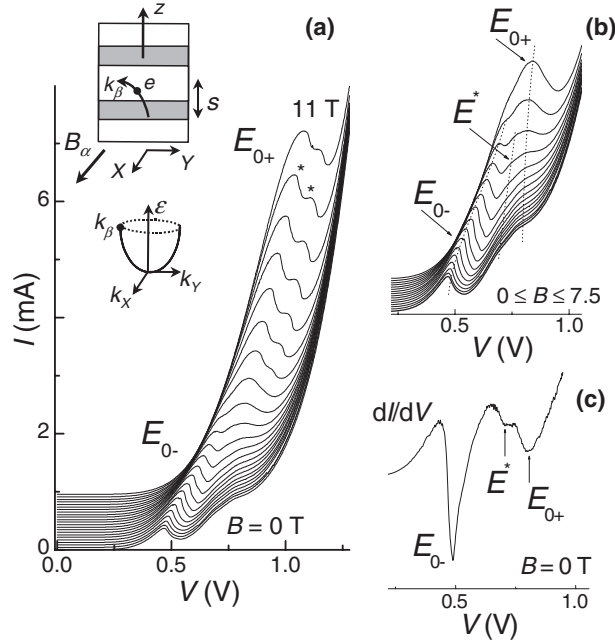
**Figure 7.** (a) $I(V)$ curves under illumination at $T = 4.2$ K and various values of $B$ for a RTD with $y = 0.08\%$. $B$ is increased from 0 to 11 T in steps of 0.5 T. For clarity, the curves are displaced along the vertical axis. The double-step decrease of $I(V)$ marked by asterisks on one of the high field curves arises from the instability in the current due to the strong negative differential conductance. The left inset is a sketch of the magneto-tunnelling experiment. (b) $I(V)$ curves with $B$ in the range 0–7.5 T. Dotted lines are guides to the eye and show resonances $E_{0-}$, $E_{0+}$ and $E^*$. (c) A differential conductance, $\mathrm{d}I/\mathrm{d}V$, plot for $B = 0$ T (from [12]).

(see figure 8(b)) [5]. This strongly supports the suggestion that $E_{0-}$ and $E_{0+}$ arise respectively from electron tunnelling into the N-induced $E_-$ and $E_+$ subbands of the GaAs$_{1-y}$N$_y$ QW layer. However, as shown in figure 8(c), the QW confinement has the effect of modifying the detailed form of the $\varepsilon(k)$ curves associated with $E_-$ and $E_+$:[2] the hybridization between the first QW subband states qw$_0$ and the N impurity level occurs at $k$-values smaller than those for bulk GaAs and leads to subbands $E_{0-}$ and $E_{0+}$ with smaller energy separation than for the bulk case. The QW confinement effect also gives rise to additional subbands, $E_{1-}$ and $E_{1+}$, arising from the hybridization of the higher energy QW subband states qw$_1$ with the N impurity level. This effect may explain the presence of the $E^*$ resonance and the form of its associated $V(B)$ curve. We attribute the weak $E^*$ resonance to electron tunnelling into the $E_{1-}$ states. As shown in figure 8(c), the energy minimum of the qw$_1$ subband is very close to the N level, which gives rise to a weak $E_{1-}$ energy dispersion as is observed for $E^*$. This indicates that the lowered dimensionality of the QW acts to modify significantly the band structure of the GaAs$_{1-y}$N$_y$ layer with respect to the bulk case. By measuring the $I(V)$ curves for different orientations

---

[2] For bulk GaAs$_{1-y}$N$_y$, we calculate the energy–wavevector dispersion curves of the $E_-$ and $E_+$ subbands by using the relation $E_{\pm}(k) = \frac{1}{2}[(E_M(k) + E_N) \pm \sqrt{(E_M(k) - E_N)^2 + 4yC_{MN}^2}]$, where $E_M(k)$ is the energy–wavevector dispersion curve of GaAs, $E_N$ is the energy position of the N-related level ($E_N = 1.725$ eV at 4.2 K) and $C_{MN}$ is the hybridization matrix element ($C_{MN} = 2.7$ eV). For the case of the GaAs$_{1-y}$N$_y$/Al$_{0.4}$Ga$_{0.6}$As QW, we use the same relation but with $E_M(k)$ equal to the energy–wavevector dispersion curve for each subband of the GaAs/Al$_{0.4}$Ga$_{0.6}$As QW.
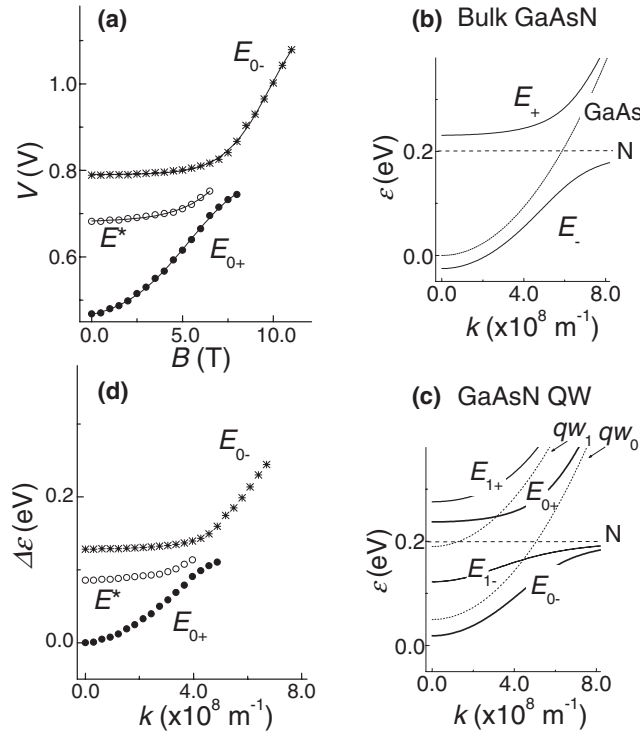
**Figure 8.** (a) The voltage position of current peaks $E_{0-}$, $E_{0+}$ and $E^*$ in $I(V)$ as a function of $B$. (b) Energy–wavevector dispersion curves for bulk $GaAs_{1-y}N_y$ (continuous curves) and for bulk GaAs (dotted lines). (c) Energy–wavevector dispersion curves for a $GaAs_{1-y}N_y$ QW (continuous curves) and for a GaAs QW (dotted curves). The energies are measured relative to the minimum of the GaAs conduction band and the N content is equal to 0.08%. (d) $\Delta\varepsilon(k)$ curves inferred from data in (a) assuming a tunnel distance $s = 40$ nm and a leverage factor $f = 2.5$ (from [12]).

of $B$ in the QW plane, we find that the voltage positions of $E_{0-}$, $E_{0+}$ and $E^*$ do not depend on the orientation of $B$ in the plane. Hence we deduce that the anisotropy in $\varepsilon(k_X, k_Y)$ for all subbands is negligible at small $k$ ($\sim B$) values.

A precise correlation between the measured $V(B)$ and $\varepsilon(k)$ curves is limited by the fact that the electrostatic leverage factor, $f$, the parameter that controls the scale of the energy values ($f = e(\mathrm{d}V/\mathrm{d}\varepsilon)$), and the value of the tunnelling distance $s$ are not known precisely. However, by using a simple electrostatic model of our device, we can estimate approximate values. We express $f$ as the ratio $d/s$, where $d$ is the distance between the edges of the doped emitter and collector layers derived from the $C(V)$ measurements ($d \sim 100$ nm) (see footnote 1). Also $d$ can be expressed as $s + d_{\mathrm{c}}$, where $d_{\mathrm{c}}$ is the distance of the centre of well from the edge of the doped collector layer ($d_{\mathrm{c}} \sim 60$ nm). This implies that $s = 40$ nm and $f = 2.5$. The value of $s$ is consistent with the structure of our device: $s$ cannot be smaller than $\sim$30 nm, since the sum of the barrier width plus the half-width of the well is 10 nm and we also need to take into account the finite spread ($\sim$20 nm) of the electron wavefunction in the emitter region adjacent to the $Al_{0.4}Ga_{0.6}As$ barrier; on the other hand, $s$ cannot be larger than 60 nm, which is the distance of the centre of well from the doped emitter layer. Figure 8(d) shows the dispersion curves $\Delta\varepsilon(k) = \varepsilon(k) - \varepsilon(0) = (V(B) - V(0))/f$ inferred from the $V(B)$ plots in figure 8(a) assuming a tunnel distance $s = 40$ nm and a leverage factor $f = 2.5$. Although the shapes of

the $\Delta\varepsilon(k)$ curves resemble those described by the band anticrossing model, we find that the energy separation between the $E_{0-}$ and $E_{0+}$ subbands is smaller ($\sim$0.13 eV) than that predicted by theory ($\sim$0.20 eV) thus suggesting a smaller value for the hybridization matrix element and/or a smaller N content in our samples than expected from the MBE growth conditions.

The $B$-dependence of the amplitude of the $E_{0-}$ and $E_{0+}$ features in $I(V)$ reveals interesting details about the nature of the $E_-$ and $E_+$ subbands. The magnitude of the tunnel current is proportional to the modulus squared of the tunnelling matrix element between the in-plane components of the emitter and QW states. At $B = 0$, the conservation of the in-plane wavevector implies that the QW states into which an electron can tunnel must have at least a partial $\Gamma$-like character, since the states of the GaAs emitter layer are almost pure $\Gamma$ states. Since $E_{0+}$ is observed at $B = 0$, we infer that the very weakly dispersed $E_+$ states have a significant $\Gamma$ conduction character even at $k = 0$. The strong enhancement of the $E_{0+}$ resonance at large $B$ and the corresponding increase of the momentum–energy dispersion at large $k$ ($k \sim B$) indicate that with increasing $k$, the $E_+$ subband states become more delocalized in real space. In contrast, the disappearance of the $E_{0-}$ resonance at large $B$ indicates that the $E_-$ subband states become strongly localized at large $k$-values. The $E^*$ feature in $I(V)$ has a similar dependence to $E_{0-}$, which confirms our assignment of this resonance to tunnelling into states of the $E_{1-}$ subband. Finally, the very weak $B$-dependence of the current features in the PC$(V)$ plots measured for samples with $y > 0.08\%$ suggest that at large $y$ the N-induced states tend to lose their $\Gamma$ character, i.e. they become increasingly localized in real space.

## 7. Conclusions

Our study reveals that for a small N content ($y = 0.08\%$) the $E_-$ and $E_+$ subbands are highly non-parabolic as expected from the BAC model and that the heavy effective mass $E_+$ states have a significant $\Gamma$ conduction band character even at $k = 0$. Our data show that the dispersion curves of the hybridized subbands of GaAs$_{1-y}$N$_y$ QW layers have a very well defined character for a small N content and suggest that the highly non-parabolic dispersion of $E_-$ and $E_+$ could be tailored by the quantum well confinement. In the devices with large $y$-values the resonances are smeared out and the measured currents are much smaller. This is attributed to the disorder in the QW and carrier trapping on localized N levels, which break the momentum conservation condition required for observing clear resonances in $I(V)$. Broad and weak current features can be observed by means of optical excitation due to the effect on the current of hole recombination with majority electrons tunnelling in resonant states of the QW. This photoinduced current enhancement provides a means of measuring the energy shift of the conduction band minimum as a function of $y$. Our study indicates that the optical absorption of GaAs$_{1-y}$N$_y$ is dominated by interband transitions involving the $E_-$ subband states. Although these are significantly energy broadened for higher $y$-values due to disorder effects, their energy position is well described by the BAC model.

## Acknowledgments

Institute, St Petersburg, Russia) and Matteo Bissiri (University of Rome 'La Sapienza', Italy) for useful discussions.

## References

[1] Sato M and Weyers M 1993 *Proc. 19th Int. Symp. GaAs and Related Compound Semiconductors (Karuizawa, 1992)* (*Inst. Phys. Conf. Ser.* vol 129) p 555
[2] Kondow M, Uomi K, Niwa A, Kitatani T, Watahiki S and Yazawa Y 1996 *Japan. J. Appl. Phys.* 1 **35** 1273
[3] Weyers M, Sato M and Ando H 1992 *Japan. J. Appl. Phys.* 2 **31** L853
[4] Hjalmarson H P, Vogl P, Wolford D J and Dow J D 1980 *Phys. Rev. Lett.* **44** 810
[5] Shan W, Walukiewicz W, Ager J W, Haller E E, Geisz J F, Friedman D J, Olson J M and Kurtz S R 1999 *Phys. Rev. Lett.* **82** 1221
[6] Lindsay A and O'Reilly E P 1999 *Solid State Commun.* **112** 443
[7] Ager J W III and Walukiewicz W (eds) 2002 *Semicond. Sci. Technol.* **17** (Special Issue: III–N–V Semiconductor Alloys) 741 and references therein
[8] Kent P R C and Zunger A 2001 *Phys. Rev.* B **64** 115208
[9] Kent P R C and Zunger A 2001 *Appl. Phys. Lett.* **79** 2339
[10] O'Reilly E P, Lindsay A, Tomic S and Kamal-Saadi M 2002 *Semicond. Sci. Technol.* **17** 870
[11] Mizuta H and Tanoue T 1995 *The Physics and Applications of Resonant Tunnelling Diodes* (Cambridge: Cambridge University Press)
[12] Endicott J, Patanè A, Ibáñez J, Eaves L, Bissiri M, Hopkinson M, Airey R and Hill G 2003 *Phys. Rev. Lett.* **91** 126802
[13] Neumann A, Patanè A, Eaves L, Belyaev A E, Gollub D, Forchel A and Kamp M 2003 Physics and technology of dilute nitrides for optical communications *IEE Proc. Optoelectron.* **150** 49
[14] Hayden R K, Maude D K, Eaves L, Valadares E C, Henini M, Sheard F W, Hughes O H, Portal J C and Cury L 1991 *Phys. Rev. Lett.* **66** 1749
[15] Beton P H, Wang J, Mori N, Eaves L, Main P C, Foster T J and Henini M 1995 *Phys. Rev. Lett.* **75** 1996
[16] Vdovin E E, Levin A, Patanè A, Eaves L, Main P C, Khanin Yu N, Dubrovskii Yu V, Henini M and Hill G 2000 *Science* **290** 122
[17] Gunn J B 1963 *Solid State Commun.* **1** 88
[18] Esaki L and Tsu R 1970 *IBM J. Res. Dev.* **14** 61
[19] Krispin P, Spruythe S G, Harris J S and Ploog K H 2002 *Appl. Phys. Lett.* **80** 2120
[20] Zhang S B and Wei S-H 2001 *Phys. Rev. Lett.* **86** 1789
[21] Leadbeater M L, Alves E S, Eaves L, Henini M, Hughes O H, Sheard F W and Toombs G A 1988 *Semicond. Sci. Technol.* **3** 1060
[22] Schubert E F, Capasso F, Hutchinson A L, Sen S and Gossard A C 1990 *Appl. Phys. Lett.* **57** 2820
[23] Yang F, Wilkinson M, Austin E J and O'Donnell K P 1993 *Phys. Rev. Lett.* **70** 323